TRANSCEIVER DESIGN FOR PRECODED MULTIPULSE MULTICARRIER PACKET TRANSMISSIONS OVER TIME-VARYING FADING CHANNELS

Manfred M. Hartmann, Gerald Matz, and Dieter Schafhuber

Institut für Nachrichtentechnik und Hochfrequenztechnik, Vienna University of Technology
Gusshausstrasse 25/389, A-1040 Vienna, Austria (Europe)
Tel.: +43 1 58801 38975; Fax: +43 1 58801 38999; Email: manfred.hartmann@nt.tuwien.ac.at

ABSTRACT

We introduce a *multipulse multicarrier (MPMC)* transceiver for packet transmissions over time-varying fading channels. The core of this system is an efficient Zak-transform implementation of the MPMC modulator/demodulator that uses optimized transmit/receive pulses. This implementation suggests a simple precoder that allows to exploit the multipath/Doppler diversity offered by the channel. The transmit symbols are recovered via an MMSE equalizer and decoder. To obtain the required channel state information, we propose efficient LS and MMSE channel estimators that are based on pilot symbols. Numerical simulations verify the diversity gain of our MPMC transceiver as well as its superiority over conventional multicarrier systems for the case of highly dispersive channels.

1. INTRODUCTION

Multipulse multicarrier (MPMC) modulation is a recently introduced wireless communication scheme that extends *multicarrier modulation* [1–3] by using multiple transmit and receive pulses [4]. In [4], algorithms and examples for the design of MPMC transmit and receive pulses have been presented. In [5], we proposed efficient MPMC system optimization algorithms and verified that in terms of spectral efficiency MPMC systems are superior to conventional multicarrier systems in the case of highly dispersive channels. In this paper, these results are complemented by the following contributions:

- We propose a packet-oriented MPMC scheme that is based on efficient Zak-Fourier domain implementations of the MPMC modulator and demodulator (Sections 2 and 3).
- We consider a simple precoding strategy that allows to exploit the diversity offered by the channel without any extra computational costs (Section 4).
- Efficient LS and MMSE channel estimators are derived which are based on regularly transmitted pilot symbols; the MPMC system is optimized such that the pulses carrying the pilots suffer from minimum interference (Sections 4 and 5).
- For data detection, we present an MMSE equalizer followed by a decoder that inverts the transmit precoding (Section 6).
- Simulation results show that our MPMC system features significant diversity gains and is superior to conventional multicarrier systems (pulse-shaping OFDM [6]) in terms of symbol error rate (SER) and channel estimation MSE (Section 7).

2. MPMC SYSTEM MODEL

The MPMC transceiver that we propose in this paper is illustrated in Fig. 1. At the transmitter, the *MPMC modulator* uses K subcarriers

Funding by FWF Grant P15156.

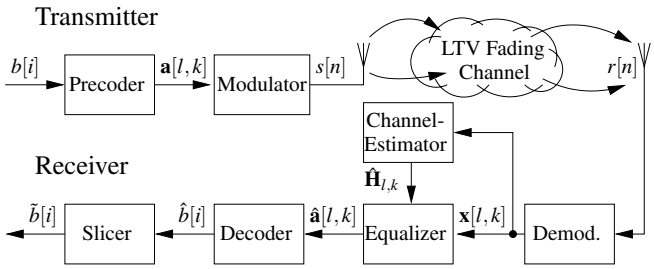

Figure 1: *Block diagram of proposed MPMC system.*

to map the symbols $a^{(r)}[l,k]$ ($l=0,\ldots,L-1$ is symbol time, $k=0,\ldots,K-1$ is the subcarrier index, $r=1,\ldots,R$ is the pulse index) to the length-N transmit signal $s[n]$ according to[1] (cf. [4])

$$s[n]=\sum_{l=0}^{L-1}\sum_{k=0}^{K-1}\mathbf{a}^T[l,k]\,\mathbf{g}_{l,k}[n],\qquad n=0,\ldots,N-1. \tag{1}$$

Here, L is the number of MPMC symbols per packet and $\mathbf{a}[l,k]\triangleq\left[a^{(1)}[l,k]\ldots\ a^{(R)}[l,k]\right]^T$. Furthermore, $\mathbf{g}_{l,k}[n]\triangleq\mathbf{g}[n-lT]\,e^{j2\pi\frac{knF}{N}}$ with $\mathbf{g}[n]\triangleq\left[g^{(1)}[n]\ldots\ g^{(R)}[n]\right]^T$ where $g^{(r)}[n]$, $r=1,\ldots,R$, denotes R linearly independent transmit pulses.[2] The symbol duration T and the subcarrier separation F are integers chosen such that

$$N=TL=KF. \tag{2}$$

The MPMC modulator is preceded by a *precoder* (see Section 4) that maps the $I\triangleq LKR$ transmit symbols $b[i]$, $i=0,\ldots,I-1$ to the symbols $a^{(r)}[l,k]$. The transmit symbols $b[i]$ are drawn i.i.d. from a finite symbol alphabet $\mathcal{A}_b$ and have zero mean and variance σ_b^2.

The packet $s[n]$ is transmitted over a *time-varying Rayleigh fading channel* $\mathbb{H}$. In terms of the channel's *spreading function* $S_{\mathbb{H}}[m,\nu]$ (m and ν denote *delay* and normalized *Doppler*, respectively), the received signal $r[n]$ equals (cf. [7] and Appendix A)

$$r[n]=(\mathbb{H}s)[n]+w[n]=\sum_{(m,\nu)\in\mathcal{S}_{\mathbb{H}}}S_{\mathbb{H}}[m,\nu]\,s[n-m]\,e^{j2\pi\frac{m\nu}{N}}+w[n]. \tag{3}$$

Here, $w[n]$ is white Gaussian noise with variance σ_w^2 and $\mathcal{S}_{\mathbb{H}}$ denotes the spreading function's support. We assume that the channel is *underspread* [8], i.e., the *channel spread* $\rho_{\mathbb{H}}\triangleq\frac{|\mathcal{S}_{\mathbb{H}}|}{N}\ll 1$, and satisfies the WSSUS assumptions (cf. [8, 9]). The second-order statistics of $\mathbb{H}$ are then characterized by the *scattering function* [8, 9] $C_{\mathbb{H}}[m,\nu]=\mathcal{E}\{|S_{\mathbb{H}}[m,\nu]|^2\}$.

[1] We use $(\cdot)^T$ to denote transposition, $(\cdot)^*$ for complex conjugation, and $(\cdot)^H$ for Hermitian transposition.

[2] Unless stated otherwise, all time-shifts are cyclic modulo N.

At the receiver, the *MPMC demodulator* uses R receive pulses $\boldsymbol{\gamma}^{(r)}[n], r = 1,\ldots,R$, to calculate the receive symbols $x^{(r)}[l,k]$ as

$$\mathbf{x}[l,k] = \sum_{n=0}^{N-1} r[n]\,\boldsymbol{\gamma}_{l,k}^{*}[n]. \tag{4}$$

Here, $\mathbf{x}[l,k] = \left[x^{(1)}[l,k]\ldots x^{(R)}[l,k]\right]^T$ and $\boldsymbol{\gamma}_{l,k}[n] = \boldsymbol{\gamma}[n-lT]\,e^{j2\pi\frac{knF}{N}}$ with $\boldsymbol{\gamma}[n] = \left[\gamma^{(1)}[n]\ldots\gamma^{(R)}[n]\right]^T$. In the case of an ideal channel ($r[n] = s[n]$), perfect symbol recovery ($\mathbf{x}[l,k] = \mathbf{a}[l,k]$) is obtained iff $\mathbf{g}[n]$ and $\boldsymbol{\gamma}[n]$ are *biorthogonal*, i.e.,

$$\sum_{n=0}^{N-1} \mathbf{g}[n]\,\boldsymbol{\gamma}_{l,k}^{H}[n] = \delta[l]\,\delta[k]\,\mathbf{I}. \tag{5}$$

If in addition $\mathbf{g}[n] = \boldsymbol{\gamma}[n]$, the MPMC system is termed *orthogonal*. It can be shown that (bi)orthogonal pulses for MPMC systems exist iff $TF/(NR) \geq 1$. Due to the Balian-Low theorem, time-frequency localized pulses moreover require $TF/(NR) > 1$ (cf. [4]). Since the spectral efficiency of MPMC systems is proportional to $NR/(TF)$, typically $TF/(NR) = 1+\varepsilon$ with small $\varepsilon > 0$.

The remainder of the MPMC receiver consists of an *equalizer* that calculates symbol estimates $\hat{\mathbf{a}}[l,k]$ from $\mathbf{x}[l,k]$, a *decoder* that inverts the precoder mapping to yield decoded symbols $\hat{b}[i]$, and a *slicer* that generates the final symbol decisions $\tilde{b}[i]$ (see Section 6). The channel coefficient matrices $\mathbf{H}_{l,k}$ (see (9) below) required by the equalizer are obtained by a channel estimator via an estimate $\hat{S}_{\mathbb{H}}[m,v]$ of the channel's spreading function using an MMSE or LS approach (see Section 5).

System Relation. Combining (1), (3), and (4) it can be shown that $\mathbf{a}[l,k]$ and $\mathbf{x}[l,k]$ are related as (cf. [5])

$$\mathbf{x}[l,k] = \sum_{l'=0}^{L-1}\sum_{k'=0}^{K-1} \mathbf{H}_{l,k;l',k'}\,\mathbf{a}[l',k'] + \mathbf{z}[l,k] \tag{6}$$

with $\mathbf{z}[l,k] = \sum_{n=0}^{N-1} w[n]\boldsymbol{\gamma}_{l,k}^{*}[n]$ and the $R\times R$ channel coefficient matrices

$$\mathbf{H}_{l,k;l',k'} = e^{j2\pi\frac{k'-k}{K}lT} \sum_{(m,v)\in\mathcal{S}_{\mathbb{H}}} S_{\mathbb{H}}[m,v] \cdot \mathbf{A}_{\boldsymbol{\gamma},\mathbf{g}}^{*}[m-(l-l')T, v-(k-k')F]\,e^{j2\pi\left(\frac{lv}{L}-\frac{k'm}{K}\right)}, \tag{7}$$

that involve the *matrix cross ambiguity function*

$$\mathbf{A}_{\boldsymbol{\gamma},\mathbf{g}}[m,v] \triangleq \sum_{n=0}^{N-1} \boldsymbol{\gamma}[n]\,\mathbf{g}^{H}[n-m]e^{-j2\pi\frac{vn}{N}}. \tag{8}$$

Eq. (6) can be rewritten as

$$\mathbf{x}[l,k] = \mathbf{H}_{l,k}\,\mathbf{a}[l,k] + \mathbf{e}[l,k], \qquad \text{with } \mathbf{H}_{l,k} \triangleq \mathbf{H}_{l,k;l,k}. \tag{9}$$

Here, we used the error vector

$$\mathbf{e}[l,k] \triangleq \sum_{(l',k')\neq(l,k)} \mathbf{H}_{l,k;l',k'}\,\mathbf{a}[l',k'] + \mathbf{z}[l,k]$$

that accounts for the noise and—via $\mathbf{H}_{l,k;l',k'}$ for $(l,k)\neq(l',k')$—for *intersymbol interference* (ISI) and *intercarrier interference* (ICI).

The idea behind (9) is to neglect[3] ISI and ICI, which allows for simple scalar equalization in the case of a conventional single-pulse multicarrier system (e.g. pulse-shaping OFDM). In the context of MPMC, (9) means that there also exists *interpulse interference* (IPI) characterized by the non-diagonal entries of $\mathbf{H}_{l,k}$. This IPI is tolerated in the pulse design and will be combated via a matrix equalizer (cf. Section 6). This idea was introduced in [5], where it was shown that MPMC systems may outperform conventional multicarrier systems in terms of spectral efficiency.

[3]Pulse optimization procedures minimizing ISI/ICI for single-pulse multicarrier systems were proposed in [6, 10–12].

3. EFFICIENT ZAK-FOURIER IMPLEMENTATION

We next present an efficient MPMC implementation based on the *piecewise discrete Zak transform* (PDZT). We restrict to MPMC systems where $TF/N = p \in \mathbb{N}$ is integer (this restriction is not severe). Extensions to rational TF/N are straightforward (cf. [5]).

Zak and Fourier Transform. We define the *discrete Zak transform* (DZT) of a length-N signal $s[n]$ as [13, 14]

$$(\mathcal{Z}s)[n,q] \triangleq \frac{1}{\sqrt{F}} \sum_{i=0}^{F-1} s[n+iK]e^{j2\pi\frac{qi}{F}}.$$

The DZT is a unitary mapping, 2-D periodic in the sense that $(\mathcal{Z}s)[n,q+F] = (\mathcal{Z}s)[n,q]$ and $(\mathcal{Z}s)[n+K,q] = e^{j2\pi\frac{n}{F}}(\mathcal{Z}s)[n,q]$, and can efficiently be computed by K length-F FFTs [14].

The PDZT of $s[n]$ is defined as the length-p vector [13]

$$(\mathcal{P}s)[n,q] \triangleq \Big[(\mathcal{Z}s)[n,q]\ (\mathcal{Z}s)[n,q+L]\ldots(\mathcal{Z}s)[n,q+(p-1)L]\Big]^T.$$

Like the DZT, the PDZT is 2-D periodic. It is a unitary mapping from the Hilbert space $l^2(\mathbb{Z}/N)$ of length-N signals to the Hilbert space $\mathcal{H}_{K,L}^{p} \triangleq l^2([0,K-1]\times[0,L-1];\mathbb{C}^p)$ of 2-D vector sequences. This means that the PDZT preserves the $l^2(\mathbb{Z}/N)$ inner product $\langle s,r\rangle \triangleq \sum_{n=0}^{N-1} r^{*}[n]\,s[n]$ in the sense that

$$\langle s,r\rangle = \langle \mathcal{P}s, \mathcal{P}r\rangle_{\mathcal{H}_{K,L}^{p}} \triangleq \sum_{n=0}^{K-1}\sum_{q=0}^{L-1} (\mathcal{P}r)^{H}[n,q]\,(\mathcal{P}s)[n,q]. \tag{10}$$

Using time-frequency shift properties of the DZT (cf. [13]), one can show that for $s_{l,k}[n] = s[n-lT]e^{j2\pi\frac{knF}{N}}$ one has

$$(\mathcal{P}s_{l,k})[n,q] = e^{-j2\pi\left(\frac{lq}{L}-\frac{kn}{K}\right)}(\mathcal{P}s)[n,q]. \tag{11}$$

We complement the PDZT with a *2-D discrete Fourier transform* (DFT) of a $R\times 1$ vector sequence $\mathbf{x}[l,k]$, defined as

$$(\mathcal{F}\mathbf{x})[n,q] \triangleq \frac{1}{\sqrt{KL}} \sum_{k=0}^{K-1}\sum_{l=0}^{L-1} \mathbf{x}[l,k]\,e^{-j2\pi\left(\frac{lq}{L}-\frac{kn}{K}\right)}. \tag{12}$$

The 2-D DFT is a unitary mapping from the Hilbert space $\mathcal{H}_{L,K}^{R}$ to the Hilbert space $\mathcal{H}_{K,L}^{R}$ with inner product as defined in (10).

MPMC Modulator. With the $R\times p$ modulator matrix

$$\mathbf{G}[n,q] \triangleq \Big[\big(\mathcal{P}g^{(1)}\big)[n,q]\ \ldots\ \big(\mathcal{P}g^{(R)}\big)[n,q]\Big]^H, \tag{13}$$

it follows from (11) and (12) that the PDZT of (1) can be written as

$$\mathbf{S}[n,q] \triangleq (\mathcal{P}s)[n,q] = \sqrt{KL}\,\mathbf{G}^{H}[n,q]\,\mathbf{A}[n,q],$$

where $\mathbf{A}[n,q] \triangleq (\mathcal{F}\mathbf{a})[n,q]$. This amounts to a simple matrix-vector multiplication for each (n,q). The transmit signal $s[n]$ is obtained as inverse PDZT of $\mathbf{S}[n,q]$. A block diagram for this Zak-Fourier domain MPMC modulator implementation is depicted in Fig. 2(a).

MPMC Demodulator. Similarly, it can be shown via (10) and (11) that the 2-D DFT of $\mathbf{x}[l,k]$ in (4) is

$$\mathbf{X}[n,q] \triangleq (\mathcal{F}\mathbf{x})[n,q] = \sqrt{LK}\,\boldsymbol{\Gamma}[n,q]\,\mathbf{R}[n,q] \tag{14}$$

with $\mathbf{R}[n,q] \triangleq (\mathcal{P}r)[n,q]$ and the $R\times p$ demodulator matrix

$$\boldsymbol{\Gamma}[n,q] = \big[\big(\mathcal{P}\boldsymbol{\gamma}^{(1)}\big)[n,q]\ \ldots\ \big(\mathcal{P}\boldsymbol{\gamma}^{(R)}\big)[n,q]\big]^H. \tag{15}$$

Again, (14) amounts to a simple matrix-vector multiplication for each (n,q). The receive symbols $\mathbf{x}[l,k]$ are obtained as 2-D inverse DFT of $\mathbf{X}[n,q]$. A block diagram for the Zak-Fourier domain MPMC demodulator implementation is depicted in Fig. 2(b).

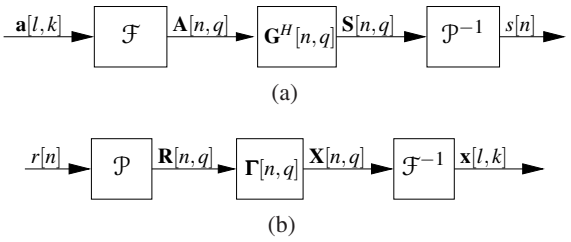

Figure 2: *Zak-Fourier implementation of (a) MPMC modulator and (b) MPMC demodulator.*

Computational Complexity. We next assess the computational complexity of MPMC (de)modulator assuming that the Zak and Fourier transforms are implemented using FFTs. Both MPMC modulator and demodulator involve KL matrix multiplications, a 2-D DFT and a PDZT (or their inverses). With $I = LKR$ symbols $b[i]$ transmitted per packet, the number of operations per transmit symbol can be shown to be $\mathcal{O}(\log_2(LK))$ for the 2-D DFT, $\mathcal{O}(\frac{p}{R}\log_2(Lp))$ for the PDZT, and $\mathcal{O}(p)$ for the matrix-vector multiplications. Therefore, complexity scales only logarithmically with the number of subcarriers (K) and MPMC symbols (L).

4. SYSTEM DESIGN

In this section, we discuss the design of the precoder in Fig. 1 and of the MPMC modulator and demodulator pulses, particularly those carrying pilot symbols dedicated for channel estimation.

Precoder Design. In multicarrier transmissions over fading channels, the symbol error rate (SER) suffers from deep fades affecting individual symbols. This effect is often combatted via diversity techniques like multicarrier CDMA [15] where each symbol is spread over several subcarriers.

In order to exploit multipath and Doppler diversity, the symbols $b[i]$ should be spread in time and frequency over several independently fading subcarriers and MPMC symbols rather than using the direct mapping $\mathbf{a}[l,k] = \mathbf{b}[k,l] \triangleq \left[b^{(1)}[k,l] \ldots\ b^{(R)}[k,l]\right]^T$ with $b^{(r)}[k,l]$, $r = 1,...,R$, $k = 1,...,K-1$, $l = 1,...,L-1$ obtained via reindexing of $b[i]$. To achieve this, we propose with some hindsight a non-redundant precoding of the transmit symbols using an inverse 2-D DFT as

$$\mathbf{a}[l,k] \triangleq (\mathcal{F}^{-1}\,\mathbf{b})[l,k]. \tag{16}$$

Hence, each symbol $b^{(r)}[l,k]$ is spread across the LK transmit pulses $g^{(r)}_{l,k}[n]$ with the same pulse index r but not across pulses with different indices $r' \neq r$. This is reasonable since the fading coefficients affecting the pulses $g^{(r)}_{l,k}[n]$, $r = 1,\ldots,R$, are highly correlated.

We conjecture that for $LK \geq |\mathcal{S}_{\mathbb{H}}|$, our precoding allows to achieve the maximum multipath-Doppler diversity. This conjecture is supported by the maximum diversity scheme in [7], which also spreads the transmit symbols over the whole time-frequency plane. A specific advantage of our precoder, however, is the fact that it cancels with the 2-D DFT of the MPMC modulator such that $\mathbf{A}[n,q] = \mathbf{b}[n,q]$ (see Fig. 2(b)). The precoder can thus be "implemented" by just omitting the 2-D DFT in the modulator and directly passing the transmit symbols $\mathbf{b}[k,l]$ to the modulation matrix, thus actually reducing the complexity of the MPMC transmitter.

Pulse Design. Pulse design aims at choosing the pulses $\mathbf{g}[n]$ and $\boldsymbol{\gamma}[n]$ such that the interference $\mathbf{e}[l,k]$ in (9) is minimized. This issue has previously been addressed in [5] where perfect channel knowledge at the receiver was assumed. In contrast to that paper, however, our goal here is to devise an MPMC system with pilot-based channel estimation. Since the information symbols are unknown at the receiver, the MPMC system should be designed such that there is negligible interference between the pulses carrying the information symbols and those carrying the pilots.

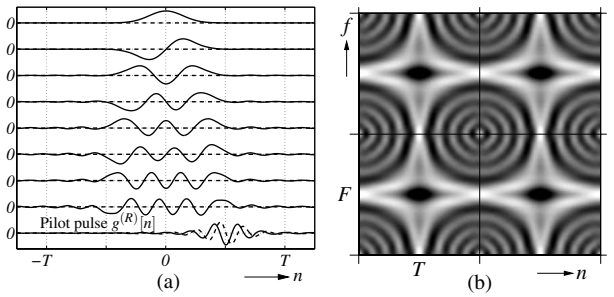

Figure 3: *MPMC system with pilots and $R = 9$: (a) optimized orthogonal pulse set, (b) time-varying power spectrum of corresponding transmit signal (darker shading corresponds to higher energy).*

To meet this objective, we propose to split the MPMC system such that the subsystems with $g^{(r)}[n]$ ($\boldsymbol{\gamma}^{(r)}[n]$), $r = 1,...,R-1$ carry the actual information symbols, while the subsystem with $g^{(R)}[n]$, $\boldsymbol{\gamma}^{(R)}[n]$ carries LK pilot symbols. The goal of having vanishing IPI on the pilots amounts to the condition $[\mathbf{H}_{l,k}]_{r,R} \approx 0$ and $[\mathbf{H}_{l,k}]_{R,r} \approx 0$ for all $r = 1,...,R-1$ (cf. (9)). While many designs may meet these criteria, we propose the following procedure that yields excellent performance (cf. [5] and Section 7): choose the first $R-1$ Hermite functions [16] as initial pulses $g^{(r)}_0[n]$, $r = 1,\ldots,R-1$ (the ratio of their temporal and spectral spread should equal T/F) and let $g^{(R)}_0[n] = g^{(1)}_0\left[n - \frac{T}{2}\right] e^{j2\pi\frac{nF}{2N}}$, i.e., the pulses carrying the pilots are time-frequency shifted Gaussians. These initial pulses are then orthogonalized (cf. [4]) and subjected to the iterative pulse optimization procedure in [5]. An example for the resulting orthogonal pulses $\mathbf{g}[n] = \boldsymbol{\gamma}[n]$ with $R = 9$ and $TF/(NR) = 1.1$ is illustrated in Fig. 3(a). Fig. 3(b) shows a section of the time-varying power spectrum [16] of the corresponding transmit signal, demonstrating that the pulses carrying the pilots are well separated.

5. CHANNEL ESTIMATION

In order to avoid aliasing, we assume that $S_{\mathbb{H}}[m,v]$ has (known) support $\mathcal{S}_{\mathbb{H}} = [m_{\min}, m_{\max}] \times [v_{\min}, v_{\max}]$ and that the channel's *delay spread* $M \triangleq m_{\max} - m_{\min} + 1$ and *Doppler spread* $V \triangleq v_{\max} - v_{\min} + 1$ satisfy $V \leq L$ and $M \leq K$. This implies that $LK \geq VM$, i.e., the number of pilots per packet (LK) must not be lower than the degrees of freedom of the channel (VM).

We next show how to estimate the channel's spreading function $S_{\mathbb{H}}[m,v]$ using the known pilot symbols $a^{(R)}[l,k]$ and the receive symbols $x^{(R)}[l,k]$. Using (10), (7) and (8), the R-th component of (9) can be written in the Zak-Fourier domain as

$$X^{(R)}[n,q] = \sum_{(m,v)\in\mathcal{S}_{\mathbb{H}}} S_{\mathbb{H}}[m,v]\,c[m,v]\,A^{(R)}[n-m,q-v] + E^{(R)}[n,q] \tag{17}$$

with $A^{(R)}[n,q] \triangleq (\mathcal{F}\,a^{(R)})[n,q]$, $X^{(R)}[n,q] \triangleq (\mathcal{F}\,x^{(R)})[n,q]$ and $E^{(R)}[n,q] \triangleq (\mathcal{F}\,e^{(R)})[n,q]$. Furthermore,

$$c[m,v] \triangleq \sum_{n=0}^{K-1}\sum_{q=0}^{L-1} \left(\mathcal{P}\,\boldsymbol{\gamma}^{(R)}\right)^H[n,q]\left(\mathcal{P}\,g^{(R)}\right)[n-m,q-v]\,e^{j2\pi\frac{vn}{N}},$$

which can be precomputed and is required only for $(m,v) \in \mathcal{S}_{\mathbb{H}}$.

Designing the pilot symbols such that

$$A^{(R)}[n,q] = \sqrt{LK}\,\delta[n-n_p]\,\delta[q-q_p]$$

for some $n_p = 0,\ldots,K-1$ and $q_p = 0,\ldots,L-1$ (e.g., $n_p = K/2$, $q_p = L/2$ amounts to $a^{(R)}[l,k] = (-1)^{l+k}$) allows to simplify (17) to

$$X^{(R)}[n,q] = S_{\mathbb{H}}[n-n_p, q-q_p]\,\sqrt{LK}\,c[n-n_p, q-q_p] + E^{(R)}[n,q]$$

Based on this simple relation, the MMSE estimate of $S_{\mathbb{H}}[m,v]$ equals

$$\hat{S}_{\mathbb{H}}[m,v] = \phi[m,v]\,X^{(R)}[m+n_p, v+q_p], \quad (m,v) \in \mathcal{S}_{\mathbb{H}}, \tag{18}$$

$$\phi[m,v] \triangleq \left(\sqrt{LK}\,c[m,v] + \frac{\sigma_e^2}{C_{\mathbb{H}}[m,v]c^*[m,v]\sqrt{LK}}\right)^{-1}. \tag{19}$$

Here, $\sigma_e^2 = \mathcal{E}\{|e^{(R)}[l.k]|^2\}$ can be calculated exactly via the channel statistics (cf. [5]) or approximated as $\sigma_e^2 \approx \sigma_w^2 \|\boldsymbol{\gamma}^{(R)}\|_2^2$ (this ignores ISI/ICI). If σ_e^2 and $C_{\mathbb{H}}[m,v]$ are unknown, a least squares (LS) estimate can be obtained with

$$\phi[m,v] \triangleq \left(\sqrt{LK}\,c[m,v]\right)^{-1}.$$

If only the scattering function support $\mathcal{S}_{\mathbb{H}}$ and the path loss $\sigma_{\mathbb{H}}^2$ are known, a robust design with performance between LS and MMSE is obtained by using $C_{\mathbb{H}}[m,v] = \sigma_{\mathbb{H}}^2/(VM)$, $(m,v) \in \mathcal{S}_{\mathbb{H}}$ in (19).

Note that with the Zak-Fourier implementation of the demodulator (cf. Fig. 2(b)), $X^{(R)}[n,q]$ is directly available. Since $\phi[m,v]$ can be precomputed, channel estimation according to (18) requires only a few multiplications.

An estimate of the coefficient matrices $\mathbf{H}_{l,k}$ in (9) is obtained via (7) by replacing $S_{\mathbb{H}}[m,v]$ with $\hat{S}_{\mathbb{H}}[m,v]$ in (18):

$$\hat{\mathbf{H}}_{l,k} = \sum_{(m,v)\in\mathcal{S}_{\mathbb{H}}} \hat{S}_{\mathbb{H}}[m,v]\,\mathbf{A}^*_{\boldsymbol{\gamma},\mathbf{g}}[m,v]\,e^{j2\pi\left(\frac{lv}{L}-\frac{km}{K}\right)}. \tag{20}$$

Note that this is an inverse 2-D DFT that can efficiently be implemented using FFTs. Further complexity reductions can be obtained by computing only a few main diagonals of $\mathbf{A}^*_{\boldsymbol{\gamma},\mathbf{g}}[m,v]$ and $\hat{\mathbf{H}}_{l,k}$. With the system design based on Hermite functions (see Section 4), the resulting band-diagonal matrices are excellent approximations. Some modifications required in practical implementations are discussed in Appendix A.

6. EQUALIZATION AND DETECTION

We next consider the problem of recovering the transmit symbols $b[i]$ from $\mathbf{x}[l,k]$. Inserting (16) in (9), we obtain

$$\mathbf{x}[l,k] = \mathbf{H}_{l,k}\,(\mathcal{F}^{-1}\mathbf{b})[l,k] + \mathbf{e}[l,k]. \tag{21}$$

The error vector $\mathbf{e}[l,k]$ is characterized by its correlation matrix $\mathbf{C_e} = \mathcal{E}\{\mathbf{e}[l,k]\,\mathbf{e}^H[l,k]\}$, which, for known $C_{\mathbb{H}}[m,v]$ and σ_w^2, can be calculated exactly (cf. [5]). Otherwise, a simple approximation ignoring ISI/ICI is given by $\mathbf{C_e} \approx \sigma_w^2 \sum_n \boldsymbol{\gamma}^*[n]\boldsymbol{\gamma}^T[n]$.

An ML detector for the symbols $b[i]$ in (21) that is optimum in terms of the SER is not feasible since its computational complexity grows exponentially with $I = LKR$. Thus, we propose a detector consisting of an equalizer and a decoder (that inverts the precoding) followed by a slicer. The LMMSE estimate of $\mathbf{b}[k,l]$ is (cf. (16))

$$\hat{\mathbf{b}}[k,l] \triangleq (\mathcal{F}\hat{\mathbf{a}})[k,l],$$

with the MMSE equalizer output

$$\hat{\mathbf{a}}[l,k] \triangleq \sigma_b^2\,\mathbf{H}_{l,k}^H\left(\sigma_b^2\mathbf{H}_{l,k}\,\mathbf{H}_{l,k}^H + \mathbf{C_e}\right)^{-1}\mathbf{x}[l,k]. \tag{22}$$

In practice the channel coefficient matrices $\mathbf{H}_{l,k}$ are replaced by $\hat{\mathbf{H}}_{l,k}$ in (20). Alternatively, ZF equalization can be achieved by setting $\mathbf{C_e} = \mathbf{0}$ in (22). Finally, the slicer quantizes the equalized, decoded and reindexed symbols $\hat{b}^{(r)}[k,l] \to \hat{b}[i]$ according to the minimum distance principle.

7. SIMULATION RESULTS

We simulated an MPMC system with $R = 9$ pulses, $K = 36$ subcarriers, packets consisting of $L = 36$ MPMC symbols, and symbol duration/subcarrier spacing $T = F = 360$. Thus, the packet length is $N = LT = 12.960$ and $p = \frac{TF}{N} = 10$. Each packet carries $I = LKR = 11.664$ 4-QAM transmit symbols of which $LK = 1296$ are pilot symbols, corresponding to a spectral efficiency of $\log|\mathcal{A}_p|\frac{R-1}{TF/N} = 1.6$ bit/s/Hz. Transmissions with and without precoding were considered. Assuming a sampling time of $T_s = 1.5\,\mu$s, the symbol duration is $540\,\mu$s, the subcarrier spacing is 18.5 kHz, and the transmission bandwidth is 667 kHz.

For comparison, we considered a pulse-shaping OFDM system (i.e., an MPMC system with $R = 1$) with orthogonalized Gaussian pulses designed according to [6], $T = 120$, $K = 108$, and $L = 108$. The packet length thus again is $N = 12.960$. Transmitting pilot symbols at the same time-frequency locations as in the $R = 9$ system again leads to a spectral efficiency of $= 1.6$ bit/s/Hz.

The channel estimator was designed for an equivalent discrete WSSUS channel with flat scattering function and $m_{\max} = -m_{\min} = 6$, $\nu_{\max} = -\nu_{\min} = 6$ (i.e., $\rho_{\mathbb{H}} = 0.01$). At carrier frequency $f_c = 2$ GHz, these values correspond to $\tau_{\max} = m_{\max}T_s = 9\mu$s and $\nu_{\max} = \nu_{\max}/(NT_s) = 308.6$ Hz (i.e., maximum velocity 46.3 m/s). The channel coefficient matrices $\mathbf{H}_{l,k}$ were approximated by band matrices with five diagonals and the MMSE equalizer used the approximation $\mathbf{C_e} \approx \sigma_w^2 \sum_n \boldsymbol{\gamma}^*[n]\boldsymbol{\gamma}^T[n]$. The actual channel used in the simulations had a flat scattering function with $\rho_{\mathbb{H}} = 3\cdot10^{-4},\ldots,\,10^{-2}$.

Fig. 4(a) shows the channel estimation MSE achieved with the MPMC system and the OFDM system versus SNR for three different channel spreads. It is seen that the MPMC system consistently outperforms the OFDM system as much as 1.2 dB (for SNR= 30 dB and channel spread 0.01). This can be explained by the fact that with the MPMC system the pilot symbols suffer from much less ISI/ICI than with the OFDM system. Fig. 4(b) compares the SER of uncoded ($\mathbf{a}[l,k] = \mathbf{b}[k,l]$) and precoded ($\mathbf{a}[l,k] = (\mathcal{F}^{-1}\mathbf{b})[l,k]$) transmissions for a channel spread $8\cdot10^{-3}$. With and without precoding, the MPMC system outperforms the OFDM system for all SNRs. Furthermore, the diversity gain of the precoded systems is apparent for SNRs larger than 10 dB.

We finally determined the signal-to-noise ratio SNR_0 required for a target SER of 1%. The results for the MPMC and OFDM system with and without precoding are depicted in Fig. 4(c) for various channel spreads. Clearly, for the MPMC system SNR_0 is always lower than for the OFDM systems. For the MPMC system, SNR_0 is also seen to be virtually independent of the channel spread. Finally, the precoding of the MPMC system results in an SNR gain of about 4.5 dB.

8. CONCLUSIONS

We proposed multipulse multicarrier (MPMC) transceivers for packet transmissions over time-varying fading channels. The system features non-redundant precoding and can efficiently be implemented in a Zak-Fourier domain. At the receiver, reliable channel state information is obtained with a pilot symbol based MMSE channel estimator. A matrix equalizer is used to combat interpulse interference. Numerical simulations verified the multipath/Doppler diversity gain achieved with the proposed precoder and showed the superiority of the MPMC system over conventional multicarrier systems (pulse-shaping OFDM) in terms of channel estimation MSE and symbol error rate.

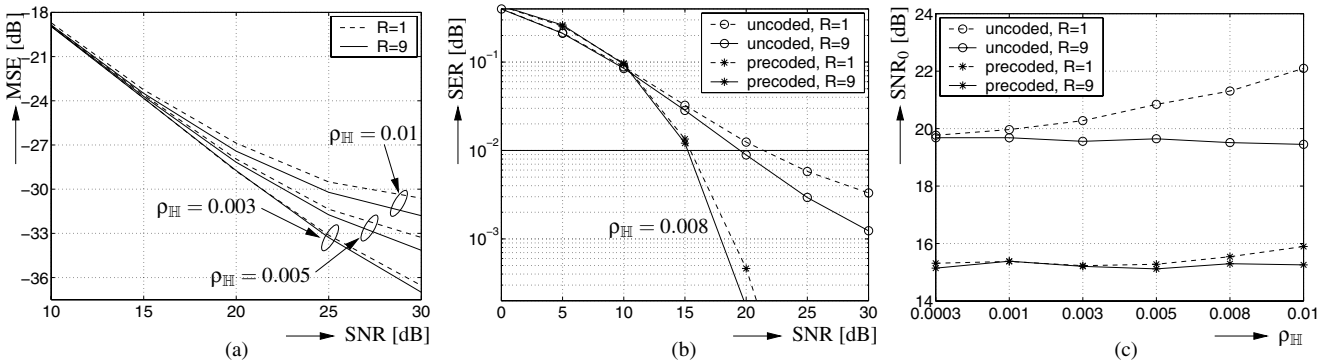

Figure 4: *Simulation results for MPMC system ($R = 9$) and pulse-shaping OFDM system ($R = 1$): (a) Channel estimation MSE versus SNR, (b) SER versus SNR at channel spread $\rho_{\mathbb{H}} = 8 \cdot 10^{-3}$, and (c) SNR required for SER$= 0.01$ versus channel spread $\rho_{\mathbb{H}}$.*

A. PRACTICAL IMPLEMENTATION ISSUES

In this appendix, we introduce two minor modifications of the proposed system that alleviate some problems resulting from imperfections of the channel model (3). In particular, practical channels do not meet the assumption of causing cyclic time-shifts. Furthermore, the length-N model (3) presupposes a time windowing which causes leakage of the spreading function in Doppler direction.

To circumvent problems with non-cyclic time-shifts, we introduce a guard interval at the beginning of each packet by setting $a^{(r)}[0,k] = 0$, $r = 1,...,R-1$. With the proposed 2-D DFT precoder this amounts to $b^{(r)}[k,0] = -\sum_{l=1}^{L-1} b^{(r)}[k,l]$, $r = 1,...,R-1$. Note that the pilot symbols $a^{(R)}[0,k]$ are localized about $n \approx T/2$ and thus can remain unaffected.

Furthermore, to avoid Doppler leakage we propose a windowing and aliasing procedure as follows. Consider a receive signal $r[n]$, $n = -dT,\ldots,N+dT-1$ where $r[0],\ldots,r[N-1]$ corresponds to the desired length-N MPMC packet and $r[-dT],\ldots,r[-1]$ and $r[N],\ldots,r[N+dT-1]$ correspond to the last/first d MPMC symbols of two neighboring packets. After the windowing $\tilde{r}[n] \triangleq r[n]\,u[n+dT]$, where $u[n]$ is a length-$(N+2dT)$ raised cosine window with roll-off d/L, a modified receive signal of length $N' = N+dT$ is obtained via the aliasing

$$r'[n] \triangleq \begin{cases} \tilde{r}[n], & n = 0,...,N-1 \\ \tilde{r}[n] + \tilde{r}[n-N-dT], & n = N,...,N+dT-1. \end{cases}$$

This is an MPMC signal with K subcarriers and $L' = L+d$ MPMC symbols, where the first L symbols are currently desired. The MPMC demodulator and the channel estimator are then implemented for packets consisting of $L+d$ MPMC symbols. Equalizer, decoder, and slicer process only the first L symbols and ignore the last d symbols. While this modification slightly increases computational complexity, it considerably improves the channel estimation performance by reducing Doppler leakage.

REFERENCES

[1] J. A. C. Bingham, "Multicarrier modulation for data transmission: An idea whose time has come," *IEEE Comm. Mag.*, vol. 28, pp. 5–14, May 1990.

[2] L. J. Cimini, "Analysis and simulation of a digital mobile channel using orthogonal frequency division multiplexing," *IEEE Trans. Comm.*, vol. 33, pp. 665–675, July 1985.

[3] Z. Wang and G. B. Giannakis, "Wireless multicarrier communications," *IEEE Signal Processing Magazine*, vol. 17, pp. 29–48, May 2000.

[4] M. M. Hartmann, G. Matz, and D. Schafhuber, "Theory and design of multipulse multicarrier systems for wireless communications," in *Proc. 37th Asilomar Conf. Signals, Systems, Computers*, (Pacific Grove, CA), pp. 492–496, Nov. 2003.

[5] M. M. Hartmann, G. Matz, and D. Schafhuber, "Multipulse multicarrier communications over time-varying fading channels: Performance analysis and system optimization," in *Proc. IEEE ICASSP-2004*, (Montreal (Canada)), pp. 805–808, May 2004.

[6] T. Strohmer and S. Beaver, "Optimal OFDM design for time-frequency dispersive channels," *IEEE Trans. Comm.*, vol. 51, pp. 1111–1122, July 2003.

[7] X. Ma and G. G. Giannakis, "Maximum-diversity transmissions over doubly selective wireless channels," *IEEE Trans. Inf. Theory*, vol. 49, pp. 1832–1840, July 2003.

[8] J. G. Proakis, *Digital Communications*. New York: McGraw-Hill, 3rd ed., 1995.

[9] P. A. Bello, "Characterization of randomly time-variant linear channels," *IEEE Trans. Comm. Syst.*, vol. 11, pp. 360–393, 1963.

[10] B. LeFloch, M. Alard, and C. Berrou, "Coded orthogonal frequency division multiplex," *Proc. IEEE*, vol. 83, pp. 982–996, June 1995.

[11] W. Kozek and A. F. Molisch, "Nonorthogonal pulseshapes for multicarrier communications in doubly dispersive channels," *IEEE J. Sel. Areas Comm.*, vol. 16, pp. 1579–1589, Oct. 1998.

[12] D. Schafhuber, G. Matz, and F. Hlawatsch, "Pulse-shaping OFDM/BFDM systems for time-varying channels: ISI/ICI analysis, optimal pulse design, and efficient implementation," in *Proc. IEEE PIMRC-02*, (Lisbon, Portugal), pp. 1012–1016, Sept. 2002.

[13] M. Zibulski and Y. Y. Zeevi, "Discrete multiwindow Gabor-type transforms," *IEEE Trans. Signal Processing*, vol. 45, pp. 1428–1442, June 1997.

[14] H. Bölcskei and F. Hlawatsch, "Discrete Zak transforms, polyphase transforms, and applications," *IEEE Trans. Signal Processing*, vol. 45, pp. 851–866, April 1997.

[15] S. Hara and R. Prasad, "Overview of multicarrier CDMA," *IEEE Comm. Mag.*, vol. 35, pp. 126–133, Dec. 1997.

[16] P. Flandrin, *Time-Frequency/Time-Scale Analysis*. San Diego (CA): Academic Press, 1999.